Desalination and Water Treatment
www.deswater.com

doi: 10.1080/19443994.2015.1085910

57 (2016) 17995–18002
August

Taylor & Francis
Taylor & Francis Group

Textile dye wastewater treatment using freshwater algae in packed-bed reactor: modeling

S. Devi[a,*], A. Murugappan[a], R. Rajesh Kannan[b]

[a]*Department of Civil Engineering, Annamalai University, Annamalai Nagar, Chidambaram, Tamil Nadu 608 002, India, Tel. +91 94864 20682; email: degisvinicivil2002@yahoo.co.in (S. Devi), Tel. +91 98424 84502; email: profam@gmail.com (A. Murugappan)*
[b]*Environmental Engineering Laboratory, Department of Chemical Engineering, Annamalai University, Annamalai Nagar, Chidambaram, Tamil Nadu 608 002, India, Tel. +91 98423 10107; email: kannan_vrr007@yahoo.com*

Received 12 December 2014; Accepted 18 August 2015

ABSTRACT

The present study was conducted for the treatment of textile dye wastewater containing reactive dye and removal of reactive blue 19 from synthetic dye solution using freshwater algae (*Spirulina platensis*) in a packed-bed up-flow column. The breakthrough curves were drawn for various bed heights (5, 7.5, and 10 cm) and flow rates (4, 8, and 12 mL/min). Several models, namely bed depth service time (BDST) model, Thomas model, Adams–Bohart model, Wolborska model, Yoon–Nelson model, Yan et al. kinetic model, and modified dose-response model were engaged to illustrate the performance of the packed-bed sorption mechanism. BDST model explained the experimental mechanism very well. The breakthrough behavior was well reported by Thomas model and Yoon–Nelson model. The optimum bed height (10 cm) and flow rate (12 mL/min) yield maximum dye uptake (251.61 mg/g). The optimal conditions were adopted for the treatment of real textile dye effluent. The biomass *S. platensis* eliminates the chemical oxygen demand, color, and turbidity of the raw wastewater than pH, total solids, suspended solids, and dissolved solids. Hence, *S. platensis* can be a successful sorbent for the treatment of wastewater containing dye.

Keywords: Reactive blue 19; Column modeling; Wastewater treatment; Freshwater algae; Packed-bed reactor

1. Introduction

Textile industry wastewater containing dyes is rich in color. This color on entering the waterways is highly visible and thus undesirable [1]. Also, dyes are carcinogenic and pose a major health hazard [2]. Reactive dyes are identified as problematic agents in the wastewater because they are water-soluble [3]. Conventional biological, unconventional methods such as UV/H_2O_2 advanced oxidation process [4] and coagulation/flocculation treatment methods are problematic in the discoloring of textile industry wastewater due to the nature of synthetic reactive dyes [5]. Recently, the curiosity increased with the use of natural and low-cost waste materials such as spent tea leaves, almond shell, wheat shells, silkworm exuviates, rice husk ash, rattan sawdust, bagasse fly ash, seashells waste, sunflower seed shells rice husk, straw, waste newspaper fiber, and sugar-extracted spent rice

*Corresponding author.

biomass [6,7] in the treatment process of dye containing wastewaters. Biological materials have shown potential for dye removal, but only low-cost biological materials with sufficiently high dye-binding capacity and selectivity for dyes are suitable for use in a full-scale biosorption process [8]. Also, sorption process will become inexpensive, if the sorbent material used is a low-cost material and does not require any expensive additional pretreatment steps [9]. The blue-green algae *Spirulina platensis* have availability in large quantities, it is largely cultivated throughout worldwide, and its annual production is about 2,000 ton [10].

In the present work, the effect of bed height and flow rate has been analyzed on sorption of reactive blue 19 onto *S. platensis* in packed-bed up-flow column. Also, this study examined the potential use of freshwater algae in treating the textile industry wastewater majorly containing reactive dyes. The optimal conditions which are used in this study (solution pH, initial dye concentration, and temperature) were acquired from batch process [11].

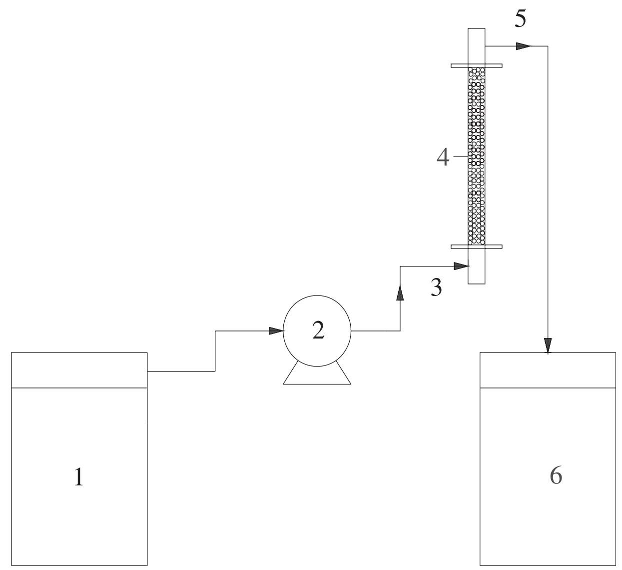

Fig. 1. Experimental setup of the packed-bed reactor.
Notes: (1) Dye effluent, (2) Peristaltic pump, (3) Inlet, (4) Packed sorbent, (5) Outlet, and (6) Treated effluent.

2. Materials and methods

2.1. Dyestuff and sorbent

The reactive blue 19 (Colour Index number: 61200) used in the adsorption experiment, was purchased from Sigma-Aldrich chemical company (Bangalore, India) and used as received. *S. platensis* was collected from the pond in Annamalai Nagar, Chidambaram. Then, it was extensively washed several times with tap water and then deionized water to get rid of soil and small aquatic organisms. Later, it was dried at room temperature for 24 h. The algal sample was ground and screened to different particle sizes. The particles of size 75–600 μm were used for sorption experiments. The FTIR spectra and SEM image of *S. platensis*, which confirm the sorption capacity of the sorbent, were presented in our earlier study [11].

2.2. Column studies

The column studies were carried out using the packed-bed column reactor. Continuous-flow experiments were conducted in an acrylic column with an internal diameter of 2.5 and 35 cm in height. The two ends of the column were connected to filter disks and plastic beads (1.5 mm in diameter) were placed at the column base in order to provide a uniform inlet flow of the solution into the column. The schematic diagram of packed-bed up-flow reactor is shown in Fig. 1.

A known quantity of sorbent was packed into the column to yield the desired bed height. Dye solution of specified concentration (250 mg/L) was pumped through the column in an upward direction at a desired flow rate using a peristaltic pump (pp15, Miclins). The optimal conditions (solution pH, initial dye concentration, and temperature) were acquired from batch process [11] and adopted for column study. The optimum pH (1.5) and temperature (30°C) was maintained. Effluent samples were collected at the column exit in certain time intervals. The concentration of centrifuged supernatant was determined using a UV double-beam spectrophotometer, (HITACHI U-2001) at a wavelength (592 nm) corresponding to the maximum optical density.

2.3. Column modeling

The modeling of the breakthrough curve was done through bed depth service time (BDST) model, Thomas model, Adams–Bohart model, Wolborska Model, Yoon–Nelson model, Yan et al. kinetic model, and modified dose-response model. These models were adopted to evaluate the effectiveness and applicability of packed-bed column for large-scale operation.

2.3.1. BDST model

BDST model is employed to calculate the bed capacity by utilizing different breakthrough values.

The observational data can be modeled by establishing a term called service time, which was set as the time taken for the effluent concentration to arrive at 1 mg/L of the dyestuff. BDST model gives a linear relationship with regard to the service time (t) and bed height (Z). The BDST model parameters can be useful to scale up the process for other flow rates without further experimental run. The equation of BDST model is given as [12]:

$$t = \frac{N_0 Z}{C_0 v} - \frac{1}{K_B C_0} \ln\left(\frac{C_0}{C_t} - 1\right) \tag{1}$$

In order to obtain the constant K_B and N_0, the plot of t against Z was developed.

2.3.2. Thomas model

Thomas [13] developed a model for adsorption processes in which external and internal diffusion limitations are not present. The Thomas model assumes plug flow behavior in the bed, and uses Langmuir isotherm for equilibrium and second-order reversible reaction kinetics.

$$\ln\left(\frac{C_t}{C_0} - 1\right) = \left(\frac{K_{Th} q_{Th} m}{Q}\right) - K_{Th} C_0 t \tag{2}$$

A plot of $\ln(C_t/C_0 - 1)$ vs. t yields the values of K_{Th} and q_{Th}.

2.3.3. Adams–Bohart model

Generally, the Adams–Bohart model [14] is used to describe the initial part of the breakthrough curve.

$$\ln\left(\frac{C_t}{C_0}\right) = K_{AB} C_0 t - K_{AB} N_0 \frac{Z}{v} \tag{3}$$

The plots of $\ln(C_t/C_0)$ vs. t was drawn to obtain the parameters K_{AB} and N_0.

2.3.4. Yoon–Nelson model

The Yoon–Nelson model is extremely concise in form, supposing that the decrease in the probability of each adsorbate to be adsorbed is proportional to the probability of its adsorption and breakthrough on the adsorbent [15]. The Yoon and Nelson equation regarding a single-component system is expressed as follows:

$$\ln\left(\frac{C_t}{C_0 - C_t}\right) = K_{YN} t - K_{YN} \tau \tag{4}$$

The values of K_{YN} and τ were calculated from the plot of $\ln(C_t/C_0 - C_t)$ vs. t.

2.3.5. Wolborska model

The Wolborska model generally describes the concentration distribution in the bed for the low concentration region (low C_t/C_0) of the breakthrough curve [16]. The expression of the Wolborska model is equivalent to the Adams–Bohart model, if the coefficient k is equal to β/N_0.

$$\ln\frac{C_t}{C_0} = \frac{\beta C_0 t}{N_0} - \frac{\beta Z}{v} \tag{5}$$

The values of β and N_0 were determined from the plot of $\ln(C_t/C_0)$ vs. t.

2.3.6. Yan et al. kinetic model

Yan et al. [17] proposed an empirical equation which could overcome the drawback in Thomas model, especially its serious deficiency in predicting the effluent concentration with respect to time zero. The empirical equation proposed by Yan et al. was found a better description of the breakthrough curves in a fixed-bed column [18].

$$\ln\left(\frac{C_t}{C_0 - C_t}\right) = \frac{K_Y C_0}{Q} \ln\left(\frac{Q^2}{K_Y q_Y m}\right) + \frac{K_Y C_0}{Q} \ln t \tag{6}$$

The K_Y and q_Y values were predicted from the plot of $\ln(C_t/C_0 - C_t)$ vs. $\ln(t)$

2.3.7. Modified dose-response model

The dose-response model [17] is based on mathematical issues instead of mechanistic fundamentals. However, its final form is similar to Thomas and Yoon–Nelson models. This model was initially developed for pharmacology studies and recently used to describe the adsorption of metals in some cases.

$$\ln\left(\frac{C_t}{C_0 - C_t}\right) = a \ln(C_0 Q t) - a \ln(q_{mdr} m) \tag{7}$$

The plot between $\ln(C_t/C_0 - C_t)$ and $\ln(C_0Qt)$ was developed to obtain values of "a" and q_{mdr}.

3. Results and discussion

3.1. Influencing variables

3.1.1. Flow rate

The consequences of flow rate on the breakthrough curves (Fig. 2) were envisaged by pumping the RB 19 dye solution of 250 mg/L concentration at different flow rates (4, 8, and 12 mL/min) through the *S. platensis*-packing column at a bed height of 5 cm. The earlier breakthrough time was achieved at higher flow rates because of minimizing contact time. The flow rate of 12 mL/min afforded the ceiling dye uptake (Table 1). Thus, the flow rate of 12 mL/min was chosen as the optimal operating condition for this system. The comparable values were accomplished for the removal of acid fuchsin using carbon–alumina composite pellet [19].

3.1.2. Bed height

The breakthrough curves were drawn (Fig. 3) to predict the influence of bed height for sorption of RB 19 onto *S. platensis* at various bed heights of 5, 7.5, and 10 cm at a flow rate of 12 mL/min. The highest sorption capacity of *S. platensis* was recorded at bed height of 10 cm. This is due to the availability of larger sorption sites. The identical phenomenon was achieved for the adsorption of acid blue 9 and basic red 29 using non-conventional sorbents in a fixed-bed column [20].

3.2. Model analysis

3.2.1. BDST model

This simplified design model ignores the intraparticle mass-transfer resistance and external film resistance such that the adsorbate is adsorbed onto the adsorbent surface directly [21]. The computed N_0 and K_B (Table 2) values are utilized to scale up the process for other flow rates without further experimental run.

The plot gave a straight line, though it does not pass through the origin. Such deviation may be caused by more than single rate-limiting step in the adsorption process [22]. The correlation between service time and bed depth for breakthrough at $C_t/C_0 = 0.1$ is shown in Fig. 4. The N_0 and K_B values are 19.52 g/L and 0.091 mL/mg min, respectively. The higher correlation coefficient value (0.923) authenticates the validation of the model with the packed-column system.

3.2.2. Thomas model

This model is suited for the adsorption processes where the external and internal diffusions will not be the limiting step [23]. When the bed height increased from 5 to 10 cm, q_{Th} increased, but the K_{Th} decreased from 0.116 to 0.052 mL/mg min. This is because the driving force for adsorption is the difference in concentration between the dye molecules on the adsorbent and in the solution [23]. Whereas the flow rate increased from 4 to 12 mL/min, the K_{Th} was increased from 0.100 to 0.116 mL/mg min. The equal experience was realized for the removal of acid blue 9 and basic red 29 using non-conventional sorbents in a fixed-bed column [20]. The greater correlation coefficient values validate the Thomas model. Moreover, a deviation was found between the experimental and predicted values of bed sorption capacity. The one and the same difference was found between the experimental and predicted values of the bed sorption capacity by the Thomas model for biosorption of Acid Blue 15 on freshwater alga *Azolla filiculoides* in column studies [24].

3.2.3. Adams–Bohart model

It is referred from Table 2 that there is no explicit pattern of constant K_{AB} while the flow rate increased. But, the bed capacity (N_0) increases with an increase in flow rate, which acknowledge the higher mass driving force. This was attributed to the availability of active sites of the adsorbents by the numerous adsorbate molecules present in higher flow of solution [25]. Poor correlation coefficient values imply the unsuitability of the Adams–Bohart model.

3.2.4. Wolborska model

Wolborska model was applied to forecast the initial part of the breakthrough curve. The predicted bed

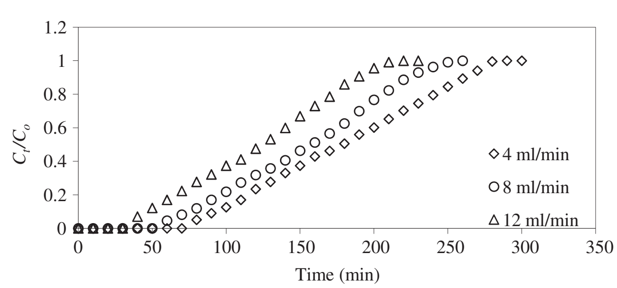

Fig. 2. Effect of flow rate on breakthrough curves for the sorption of RB 19 onto *S. platensis*.

Table 1
Sorption performance of *S. platensis* in packed-bed column for the removal RB 19 for various flow rates (bed height—5 cm) and bed heights (12 mL/min)

Flow rate (mL/min)	Bed height (cm)	Sorbent mass (g)	Volume (L)	Dye mass (mg)	Dye uptake (mg/g)
4	5	3.5	1.08	270	77.14
8	5	3.5	1.84	460	131.43
12	5	3.5	2.40	600	171.43
12	7.5	5.05	4.44	1,110	219.80
12	10	6.2	6.24	1,560	251.61

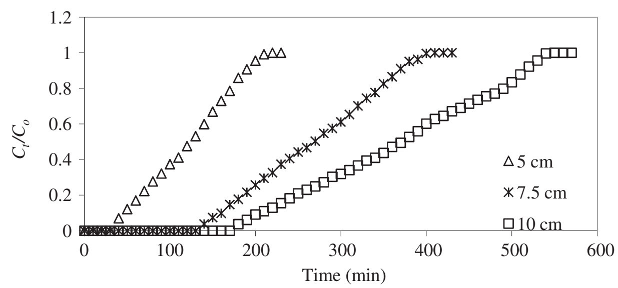

Fig. 3. Effect of bed height on breakthrough curves for the sorption of RB 19 onto *S. platensis*.

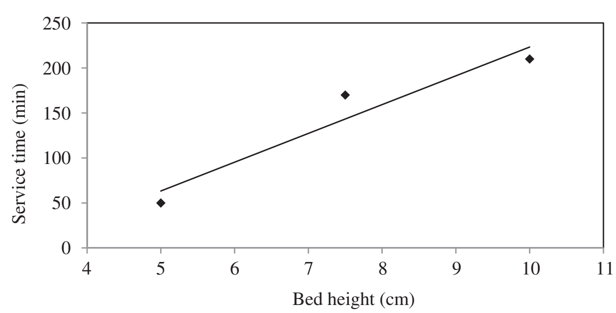

Fig. 4. BDST Model for the sorption of RB 19 onto *S. platensis* (Q—12 mL/min, v—2.44 cm/min).

capacity (N_0) by the Wolborska model was same as the value of the Adams–Bohart model. It is observed that the Wolborska model fails to accommodate the experimental data (Figure not shown). Therefore, the Wolborska model is not a valid model to represent the sorption of reactive blue 19 on *S. platensis* in packed-bed up-flow column.

3.2.5. Yoon–Nelson model

From the results, the K_{YN} value decreased from 0.029 to 0.013 min^{-1} and the τ value increased from 122.27 to 381.31 min when the bed height was increased from 5 to 10 cm. Whereas, the time required for 50% breakthrough τ value decreased from 179.04 to 122.27 min when the flow rate was increased from 4 to 12 mL/min because the saturation of the column occurs more rapidly [26]. The Yoon–Nelson rate constant (K_{YN}) increases with an increase in flow rate. Because passing dye molecules through sorbent is more at higher flow rate that increases the sorption rate [20]. The outcome is in correspondence with the removal of lead(II) using oil palm fiber in packed-bed column [27]. The higher R^2 values authorize the fitness of the Yoon–Nelson model for the overall kinetics of the column.

Table 2
Model parameters of breakthrough curve

Bed height (cm)	Flow rate (mL/min)	$q_{0(exp)}$ mg/g	Thomas model			Adams–Bohart model			Wolborska model		
			K_{Th} (mL/mg min)	q_{Th} (mg/g)	R^2	K_{AB} (mL/mg min)	N_0 (g/L)	R^2	β (l/min)	N_0 (g/L)	R^2
5	4	77.14	0.100	51.54	0.978	0.048	10.61	0.871	0.509	10.61	0.871
5	8	131.43	0.112	90.18	0.983	0.056	18.01	0.887	1.008	18.01	0.887
5	12	171.43	0.116	104.81	0.982	0.054	23.02	0.905	1.243	23.02	0.905
7.5	12	219.80	0.084	161.10	0.962	0.036	32.45	0.859	1.168	32.45	0.859
10	12	251.61	0.052	188.67	0.970	0.028	30.52	0.880	0.854	30.52	0.880

Table 3
Model parameters of breakthrough curve

			Yoon–Nelson model			Yan et al. kinetic model			Modified dose-response model		
Bed height (cm)	Flow rate (mL/min)	$q_{0(\text{exp})}$ (mg/g)	K_{YN} (1/min)	τ (min)	R^2	K_Y (mL/mg min)	q_Y (mg/g)	R^2	a	q_{mdr} (mg/g)	R^2
5	4	77.14	0.025	179.04	0.978	0.065	115.92	0.960	4.10	47.55	0.960
5	8	131.43	0.028	157.82	0.983	0.125	205.06	0.946	3.92	80.24	0.946
5	12	171.43	0.029	122.28	0.982	0.148	295.69	0.923	3.09	91.51	0.923
7.5	12	219.80	0.021	271.19	0.962	0.259	276.26	0.935	5.40	149.11	0.935
10	12	251.61	0.013	381.31	0.970	0.221	365.49	0.948	4.62	168.65	0.948

Table 4
Textile dye wastewater treatment with *S. platensis*

	Sample-1 (raw wastewater before adjusting pH)		Sample-2 (raw wastewater after adjusting pH)	
Parameters	Before treatment	After treatment	Before treatment	After treatment
COD (mg/L)	5,120	784	4,850	698
Turbidity (NTU)	28.9	20	55.1	38.9
pH	9.5	8.5	1.5	1.0
Total solids (mg/L)	4,900	4,200	4,450	3,850
Dissolved solids (mg/L)	4,350	3,750	3,950	3,500
Suspended solids (mg/L)	550	450	500	350

3.2.6. Yan et al. kinetic model

The initial stage of the model curve was fitted well with the data than the later stage. The q_Y value increases with an increase in flow rate and bed height. The analogous trend was identified for the sorption of molybdenum(VI) from aqueous solution by marine algae *Cystoseria indica* [26]. The lower R^2 values and over estimation of sorption capacity grant unfitness of the Yan et al. model to the experimental data.

3.2.7. Modified dose-response model

The predicted model breakthrough curves at initial stage were found to be fine. The "a" value was decreased with an increase in flow rate (Table 3). In contrast, the value of q_{mdr} is vice versa. The predicted q_{mdr} values (Table 3) are much lower than the experimental value and fairly similar to q_{Th}. The modified dose-response model does not adequately validate the sorption of RB 19.

3.3. Real textile industry wastewater treatment

Real textile industry wastewater containing reactive dyes was collected from the equalization ponds of a textile mill. The raw wastewater of non-adjusted pH and adjusted pH (optimum) are named as sample-1 and sample-2, respectively. The sample was pumped through the column of *S. platensis*, in an upward direction at an optimum flow rate (12 mL/min) at an optimum packed-column bed height of 10 cm. Effluent samples were collected up at the column exit. The parameters chemical oxygen demand (COD), turbidity, total solids, suspended solids, dissolved solids, and pH were tested before and after treatment for both samples. The sorbent has the capacity to remove COD of the sample-1 and sample-2 of 84.68 and 85.6%, respectively (Table 4). On the other hand, it brings down the total solids, dissolved solids, and suspended solids about 11.3 to 30%. The dark blue color of the samples became clear and colorless under optimum conditions. But, there is no evident alteration in pH of both the samples after treatment. However, the turbidity of both samples was reduced nearly 30%. Hence, it is concluded that the biomass *S. platensis* could be used as an effective sorbent in textile dye industry wastewater treatment or wastewater containing dye.

4. Conclusions

The sorption capacity of freshwater algae *S. platensis* was tested on sorption of reactive blue 19 from synthetic dye solution and raw textile industry wastewater. It is a low-cost and naturally available biomass. The higher dye uptake was recorded at the highest bed height (10 cm) and the highest flow rate (12 mL/min). The BDST model, Thomas model, and Yoon–Nelson model validate well with the breakthrough curves of the experimental system among the models used. The COD of the raw wastewater was treated up to 85.6% at optimum pH. Besides, the color and turbidity were removed at some point. The outcome of the present investigation exposed that the biomass *S. platensis* can be a successful sorbent and capable of treating textile industry wastewater as well as reactive dye from aqueous solution.

Nomenclature

a	—	modified dose-response model parameter
β	—	kinetic coefficient of external mass transfer (mL/min)
C_0	—	initial solution concentration (mg/L)
C_t	—	breakthrough dye concentration (mg/L)
K_{AB}	—	Adam–Bohart model constant (mL/mg min)
K_B	—	rate constant of BDST model (mL/mg min)
K_{Th}	—	Thomas model constant (mL/mg min)
K_Y	—	kinetic rate constant for Yan Model (mL/min/mg)
K_{YN}	—	rate constant of Yoon–Nelson model (l/min)
m	—	mass of adsorbent (g)
N_0	—	sorption capacity of bed (mg/L)
q_{mdr}	—	predicted adsorption capacity by modified dose-response model (mg/g)
q_{Th}	—	predicted adsorption capacity by Thomas model (mg/g)
q_Y	—	predicted adsorption capacity by Yan model (mg/g)
Q	—	influent flow rate (mL/min)
τ	—	time required for 50% adsorbate breakthrough (min)
v	—	linear velocity (cm/min)
Z	—	bed depth (m)

References

[1] Y. Al-Degs, M.A.M. Khraisheh, S.J. Allen, M.N. Ahmad, G.M. Walker, Competitive adsorption of reactive dyes from solution: Equilibrium isotherm studies in single and multisolute systems, Chem. Eng. J. 128 (2007) 163–167.

[2] R. Jayaraj, P.J. Thanaraj, S.T. Natarajan, P.M.D. Prasath, Removal of congo red dye from aqueous solution using acid activated eco friendly low cost carbon prepared from marine algae *Valoria bryopsis*, J. Chem. Pharm. Res. 3(3) (2011) 389–396.

[3] D. Djordjevic, D. Stojkovic, N. Djordjevic, M. Smelcerovic, Thermodynamics of reactive dye adsorption from aqueous solution on the ashes from city heating station, Ecol. Chem. Eng. S 18(4) (2011) 527–536.

[4] A. Zuorro, R. Lavecchia, Evaluation of UV/H_2O_2 advanced oxidation process (AOP) for the degradation of diazo dye Reactive Green 19 in aqueous solution, Desalin. Water Treat. 52(7–9) (2014) 1571–1577.

[5] M.S. Chiou, W.S. Kuo, H.S. Li, Removal of reactive dye from wastewater by adsorption using ECH cross-linked chitosan beads as medium, J. Environ. Sci. Health, Part A 38(11) (2003) 2621–2631.

[6] A. Zuorro, M.L. Santarelli, R. Lavecchia, Tea waste: A new adsorbent for the removal of reactive dyes from textile wastewater, Adv. Mater. Res. 803 (2013) 26–29.

[7] D. Suteu, T. Malutan, Industrial cellolignin wastes as adsorbents for removal of methylene blue dye from aqueous solutions, Bioresources 8(1) (2013) 427–446.

[8] E. Klimiuk, K. Kabardo, Z. Gusiatin, U. Filipkowska, The adsorption of reactive dyes from mixtures containing surfactants onto chitin, Pol. J. Environ. Stud. 14 (6) (2005) 771–780.

[9] R. Srivastava, D.C. Rupainwar, A comparative evaluation for adsorption of dye on neem bark and mango bark powder, Indian J. Chem. Technol. 18 (2011) 67–75.

[10] A. Çelekli, M. Yavuzatmaca, Predictive modeling of biomass production by *Spirulina platensis* as function of nitrate and NaCl concentrations, Bioresour. Technol. 100 (2009) 1847–1851.

[11] S. Devi, A. Murugappan, R. Rajesh Kannan, Sorption of Reactive blue 19 onto freshwater algae and seaweed, Desalin. Water Treat. 54 (2015) 2611–2624.

[12] S. Alvarez, J.L. Sotelo, G. Ovejero, A. Rodriguez, J. Garcia, Low-cost adsorbent for emerging contaminant removal in fixed-bed columns, Chem. Eng. Trans. 32 (2013) 61–66.

[13] H.C. Thomas, Heterogeneous ion exchange in a flowing system, J. Am. Chem. Soc. 66 (1944) 1466–1664.

[14] G. Bohart, E.Q. Adams, Some aspects of the behavior of charcoal with respect to chlorine, J. Am. Chem. Soc. 42 (1920) 523–544.

[15] Y.H. Yoon, J.H. Nelson, Application of gas adsorption kinetics I. A theoretical model for respirator cartridge service life, Am. Ind. Hyg. Assoc. J. 45 (1984) 509–516.

[16] A. Wolborska, Adsorption on activated carbon of p-nitrophenol from aqueous solution, Water Res. 23 (1989) 85–91.

[17] G.Y. Yan, T. Viraraghavan, M. Chen, A new model for heavy metal removal in a biosorption column, Adsorpt. Sci. Technol. 19 (2001) 25–43.

[18] F. Zeinali, A.A. Ghoreyshi, G.D. Najafpour, Adsorption of dichloromethane from aqueous phase using granular activated carbon: Isotherm and breakthrough curve measurements, middle East, J. Sci. Res. 5(4) (2010) 191–198.

[19] M. Dutta, J.K. Basu, Fixed-bed column study for the adsorptive removal of acid fuchsin using carbon–alumina composite pellet, Int. J. Environ. Sci. Technol. 11 (2014) 87–96.

[20] P. Sivakumar, P.N. Palanisamy, Packed bed column studies for the removal of acid blue 9 and basic red 29 using non-conventional sorbents, Indian J. Chem. Technol. 16 (2009) 301–307.

[21] R. Han, D. Ding, Y. Xu, W. Zou, Y. Wang, Y. Li, L. Zou, Use of rice husk for the adsorption of congo red from aqueous solution in column mode, Bioresour. Technol. 99 (2008) 2938–2946.

[22] K. Low, C. Lee, B. Tan, Quaternized wood as sorbent for reactive dyes, Appl. Biochem. Biotechnol. 87 (2000) 233–246.
[23] Z. Aksu, F. Gönen, Biosorption of phenol by immobilized activated sludge in a continuous packed bed: Prediction of breakthrough curves, Process Biochem. 39 (2004) 599–613.
[24] T.V.N. Padmesh, K. Vijayaraghavan, G. Sekaran, M. Velan, Biosorption of Acid Blue 15 using fresh water macroalga *Azolla filiculoides*: Batch and column studies, Dyes Pigm. 71 (2006) 77–82.
[25] N. Azouaou, Z. Sadaoui, H. Mokaddem, Removal of lead from aqueous solution onto untreated coffee grounds: A fixed-bed column study, Chem. Eng. Trans. 38 (2014) 151–156.
[26] F. Kafshgari, A.R. Keshtkar, M.A. Mousavian, Study of Mo(VI) removal from aqueous solution: Application of different mathematical models to continuous biosorption data, Iran. J. Environ. Health 10(14) (2013) 1–14.
[27] J.T. Nwabanne, P.K. Igbokwe, Adsorption performance of packed bed column for the removal of lead(II) using oil palm fibre, Int. J. Appl. Sci. Technol. 2(5) (2012) 106–115.